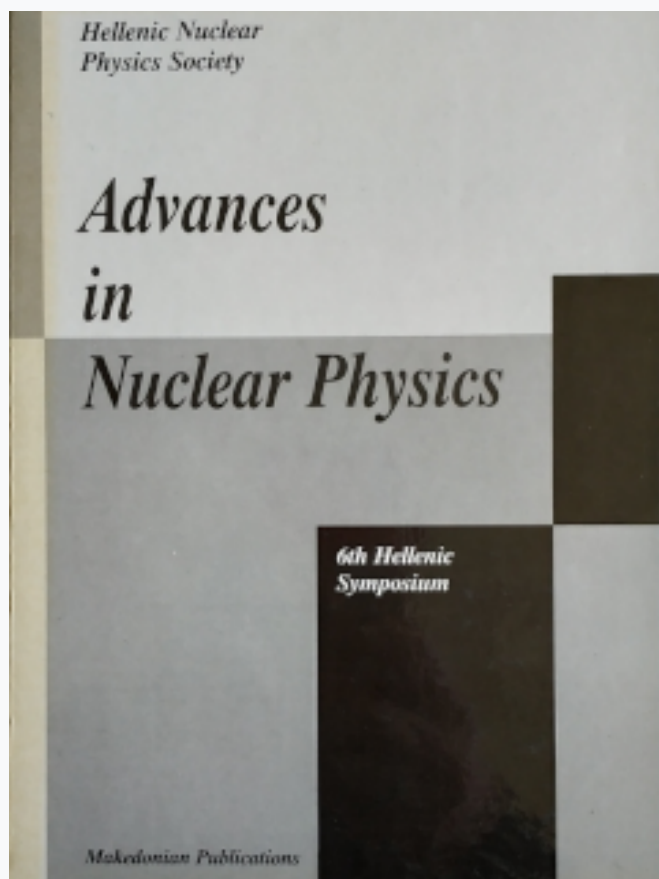


HNPS Advances in Nuclear Physics

Vol 6 (1995)

HNPS1995



Neutrino - Nucleus Reaction Cross Sections at Low and Intermediate Energies

T. S. Kosmas, E. Oset

doi: [10.12681/hnps.2919](https://doi.org/10.12681/hnps.2919)

To cite this article:

Kosmas, T. S., & Oset, E. (2020). Neutrino - Nucleus Reaction Cross Sections at Low and Intermediate Energies. *HNPS Advances in Nuclear Physics*, 6, 100–110. <https://doi.org/10.12681/hnps.2919>

Neutrino - Nucleus Reaction Cross Sections at Low and Intermediate Energies

T. S. Kosmas ^{a,1} and E. Oset ^b

^a *Division of Theoretical Physics, University of Ioannina, GR-451 10 Ioannina, Greece*

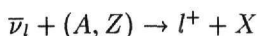
^b *Departamento de Fisica Teorica and IFIC, Centro Mixto Universidad de Valencia, CSIC, 46100, Burjassot (Valencia), Spain*

Abstract

Neutrino-nucleus reactions at low and intermediate energies up to $E_\nu = 500 \text{ MeV}$ are investigated for the most interesting nuclei from an experimental point of view. We mainly focus on calculations of neutrino-nucleus cross sections for semi-inclusive processes, for which recent measurements from radiochemical experiments at LAMPF and KARMEN have been obtained. Inclusive cross sections are also calculated and discussed. The method employed uses the Lindhard function for the description of the particle-hole excitations of the final nucleus via a local density approximation.

1 Introduction

The fundamental role which play the neutrinos in various astrophysical phenomena has been found a special experimental and theoretical interest by many authors in the last years [1-5]. For terrestrial observations of astrophysical neutrinos, i.e. solar-, supernova-, atmospheric-neutrinos etc., some favorable nuclear isotopes have been used or proposed to be used as neutrino detectors via the neutrino-nucleus reactions



where $l = e, \mu$. For these reactions, reliable estimates of neutrino-nucleus cross section for E_ν up to a few hundred MeV and especially for semi-inclusive

¹ Presented by T. S. Kosmas

and inclusive processes are very important [3-5]. For the special type of the ongoing radiochemical experiments, which register events from only particle-bound states of the final nucleus, semi-inclusive cross sections for ^{37}Cl , at Davis experiment, and for ^{71}Ga , at GALLEX and SAGE experiments are needed. Also, for reactions of neutrinos with some isotopes proposed as promising nuclear targets in neutrino detectors, like ^{81}Br , ^{98}Mo , ^{115}In , ^{127}I , ^{205}Tl , the knowledge of a reliable cross section calculation is a fundamental prerequisite [6-13]. We mention that in the case of the Cerenkov or liquid scintillation experiments we need inclusive cross sections for much higher energies than those of the radiochemical type experiments.

A thorough discussion of the various methods used so far [14-16] for neutrino nucleus cross section calculations has been done in ref. [5]. In the context of the method used in the present work, the differential neutrino nucleus cross section is expressed in terms of the local Fermi momentum $p_F(r)$. In this way both bound as well as excited states of the proton and neutron are taken into account by using the particle-hole excitations included in a relativistic Lindhard function. This function, primarily constructed for the infinite nuclear matter, has been modified [4] so as to take into account the gap for a minimum excitation energy of the final nucleus (see sect. 3).

The method used here is also appropriate to give the cross sections for particle-bound nuclear states with which the "flux averaged cross section" $\bar{\sigma}$ for radiochemical experiments can be calculated. This is experimentally a very important quantity. In the present work we have calculated the flux averaged cross sections for ν_e and ν_μ neutrinos and compared them with the corresponding values found for various electron- and muon-neutrino reactions in the KARMEN [8,9] and LAMPF [10-13] collaborations. The cross section $\bar{\sigma}$ is obtained by folding the ordinary neutrino cross sections with an appropriate energy distribution of the outgoing lepton (see sect. 4).

We have also studied total neutrino-nucleus cross sections for the most important neutrino detection nuclear isotopes for low and intermediate energies $20\text{MeV} \leq E_\nu \geq 500\text{MeV}$. These neutrino-energies, which cover the high energy supernova neutrinos, the solar flare neutrinos etc., can excite a great number of nuclear states such that, the integration over the continuum involved in the method used here is a very good approximation.

2 Description of the method

The construction of the effective Hamiltonian which describes processes (1) has been done in ref. [4]. By assuming local density approximation the total neutrino-nucleus reaction cross section σ , is written as [5]

$$\sigma = -\frac{2G^2 \cos^2 \theta_c}{\pi} \int_0^R r^2 dr \int_{p_l^{min}}^{p_l^{max}} p_l^2 dp_l \int_{-1}^1 d(\cos \theta) \frac{1}{E_\nu E_l} \bar{\sum} \sum |T|^2$$

$$\times \text{Im} \bar{U}(E_\nu - E_l - Q + Q_{th} - V_C(r), \mathbf{q}) \Theta(E_l + V_C(r) - m_l) \quad (2)$$

where the quantity $\bar{\sum} \sum |T|^2$ represents the sum and average over final and initial spins of the leptons and nucleons (see appendix of ref. [5]). The function $\Theta(E_l + V_C(r) - m_l)$ is the *theta* function, V_C is the Coulomb energy of the lepton and Q is the *Q*-value of the process. The function $\text{Im} \bar{U}(q^0, \mathbf{q})$ represents the imaginary part of the modified Lindhard function [17]. The minimum ($p_l^{min} = 0$) and maximum ($p_l^{max} = ((E_l^{max})^2 - m_\mu^2)^{1/2}$) lepton momentum are determined by the kinematics i.e.

$$E_l^{max} = E_\nu - V_C(r) - Q, \quad (3)$$

The quantity Q_{th} in eq. (2) is the difference of the proton and neutron local Fermi energies

$$Q_{th} = E_{p_F} - E_{n_F} \quad (4)$$

The magnitudes of the momenta p_{F_n} and p_{F_p} are given in terms of the neutron and proton nuclear densities, via a local density approximation. In our convention q^2 is written as

$$q^2 = q^\mu q_\mu = q_0^2 - \mathbf{q}^2 = (E_l - E_\nu)^2 - (\mathbf{p}_l - \mathbf{p}_\nu)^2 \quad (5)$$

where \mathbf{p}_i denotes the three-momentum of the particles involved in the process.

3 The use of the modified Lindhard function

In the infinite nuclear matter the gap for a minimum excitation is zero but in the case of a finite nuclear system this gap varies from $\approx 6 \text{ MeV}$, for light nuclei, to $\approx 1 - 3 \text{ MeV}$, for heavy nuclei. The sensitivity of the results on the minimum excitation energy (gap) of the participating nucleus is studied in table 1, for the total cross sections and in table 2, for the radiochemical ones.

As has been discussed in ref. [4], the use of the modified Lindhard function $\bar{U}(q^0, \mathbf{q})$ becomes necessary when studying the neutrino cross sections at low energies. The reason for it is that, the ordinary Lindhard function [18-21] for p, n excitation given by

$$\bar{U}(q^0, \mathbf{q}) = 2 \int \frac{d^3 p}{(2\pi)^3} \left\{ \frac{n(\mathbf{p})[1 - n(\mathbf{p} + \mathbf{q})]}{q^0 + \varepsilon(\mathbf{p}) - \varepsilon(\mathbf{p} + \mathbf{q}) + i\epsilon} + \frac{n(\mathbf{p})[1 - n(\mathbf{p} - \mathbf{q})]}{-q^0 + \varepsilon(\mathbf{p}) - \varepsilon(\mathbf{p} - \mathbf{q}) + i\epsilon} \right\} \quad (6)$$

where $n(\mathbf{p})$ is the occupation number of the Fermi sea and $\varepsilon(\mathbf{p})$ the nucleon kinetic energy, has a pathological behaviour at $q^0 = 0$ and $\mathbf{q} \rightarrow 0$ for the following reason.

When $q^0 = 0$ and in the limit of $\mathbf{q} \rightarrow 0$, eq. (6) leads to an expression of the type 0/0 which has a finite limit, and actually $|Re\bar{U}(0, q \rightarrow 0)|$ has a maximum there. However, the response function for a finite nucleus with closed shells is zero, since one has matrix elements of the type $\langle n | e^{i\mathbf{q} \cdot \mathbf{r}} | 0 \rangle$, with $|0\rangle$ the ground state and $|n\rangle$ standing for excited states. This matrix element vanishes for $\mathbf{q} \rightarrow 0$. Hence the disagreement between nuclear matter and finite nuclei in this limit is extreme. Actually, the numerator of eq. (6) vanishes when $\mathbf{q} \rightarrow 0$. The difference between a Fermi sea and the finite nucleus is that the denominator of eq. (6) vanishes when $q^0 = 0$ and $\mathbf{q} \rightarrow 0$, while in finite nuclei it does not. This is because in nuclear matter one has a continuum of states while in finite nuclei there is a minimum energy needed to excite the first excited state. This energy gap is what makes the denominator of the response function different of zero for finite nuclei.

Table 1. Inclusive (total) cross sections (all accessible final states contribute) for ν_e -nucleus reactions obtained by using various values of the minimum excitation energy Δ in the modified Lindhard function. (σ_{tot} in 10^{-38} cm^2).

E_ν (MeV)	σ_{tot} for $^{37}Cl(\nu_e, e^-)^{37}_{18}Ar$			σ_{tot} for $^{205}Tl(\nu_e, e^-)^{205}_{81}Pb$		
	1 MeV	3 MeV	6 MeV	1 MeV	3 MeV	6 MeV
30	0.01538	0.01249	0.01260	0.13902	0.10751	0.10882
50	0.06968	0.05456	0.05074	0.49621	0.37060	0.34424
100	0.50260	0.45194	0.41399	2.96007	2.60926	2.36321
150	1.53978	1.46552	1.39360	8.67884	8.22220	7.78100
200	3.14425	3.05769	2.96632	17.56398	17.03447	16.47959
250	5.03576	4.94517	4.84223	28.08149	27.52524	26.90237
300	6.92839	6.83780	6.72994	38.57010	38.01504	37.36728

Table 2. *Semi-inclusive (radiochemical) cross sections (particle-bound states only contribute) for ν_e -nucleus reactions obtained by using various values of the minimum excitation energy Δ in the modified Lindhard function. (σ_{rad} in 10^{-38} cm^2).*

E_ν (MeV)	σ_{rad} for $^{37}\text{Cl}(\nu_e, e^-)^{37}_{18}\text{Ar}$			σ_{rad} for $^{205}\text{Tl}(\nu_e, e^-)^{205}_{81}\text{Pb}$		
	1 MeV	3 MeV	6 MeV	1 MeV	3 MeV	6 MeV
30	0.01262	0.01121	0.01144	0.06079	0.05934	0.06268
50	0.03448	0.03291	0.03315	0.11165	0.11196	0.11700
100	0.08915	0.08791	0.08927	0.21410	0.21718	0.22578
150	0.11862	0.11787	0.11960	0.32257	0.32591	0.33387
200	0.16355	0.16333	0.16487	0.34087	0.34320	0.34975
250	0.13014	0.13022	0.13199	0.41679	0.41907	0.42770
300	0.13035	0.12987	0.13161	0.51134	0.51114	0.52125

In order to cure this pathological behaviour of the Lindhard function in the case of finite nuclear systems, this function was modified [17] by introducing a parameter Δ in the denominator of eq. (6) which accounts for the gap of the first excited state. In this way, the numerical difficulties appeared in the evaluation of the neutrino cross section at low energies for some nuclei are removed.

The pathologies disappear throughout the periodic table as soon as a gap of around 1 MeV is used and the results are then not much sensitive to the precise value of the gap used (see tables 1 and 2). Since the purpose of the gap is to avoid the numerical instabilities, in ref. [4] we have used a constant value for the gap, rather than using a precise value for each nucleus. For this value we have chosen 3 MeV, which already provides very stable results. As an example, taking instead a gap of 6 MeV changes the cross sections below the level of 2% in all the range of energies and nuclei studied for both inclusive and semi-inclusive processes (see tables 1 and 2).

4 Cross sections calculations

4.1 Total and radiochemical cross sections

In the present work we study inclusive and semi-inclusive neutrino and antineutrino-nucleus cross sections throughout the periodic table by using eq. (2).

The common characteristics of the total cross sections found in ref. [4] is that they rise appreciably at low energies but the growth becomes moderate at higher energies. In the same nucleus there are differences between the neutrino and antineutrino reactions but for each target the electron neutrino cross sections in the region $300 \leq E_\nu \leq 500 \text{ MeV}$ are about equal to the corresponding muon-neutrino cross sections and the electron antineutrino cross sections are about equal to those of the muon antineutrino.

In order to be able to calculate the radiochemical cross section we have modified the formalism of ref. [5] in such a way that the contribution of nuclear excited states above the threshold energies for proton or neutron emission E_{thres}^N is excluded. This was done by setting the integrand of eq. (2) to zero when

$$E_\nu - E_e > Q + E_{thres}^N + V_C \quad (7)$$

whith E_{thres}^N , the smallest of the values E_{thres}^p , E_{thres}^n , for proton or neutron emission.

4.2 Averaged cross section $\bar{\sigma}$

The neutrino beams used in experiments (e.g. at LAMPF, KARMEN etc.) are not monochromatic, but they present an energy distribution. In the electron neutrino case, the neutrinos are produced from the decay of muons resulting from the decay of slow pions and therefore they have relatively low energies. The energy distribution of such neutrinos is approximately described by (Michel distribution)

$$\frac{dN_\nu}{dE_\nu} \equiv W(E_\nu) \approx E_\nu^2(E_\nu^{\max} - E_\nu) \quad (8)$$

where

$$E_\nu^{\max} \approx \frac{m_\mu^2 - m_e^2}{2m_\mu} \quad (9)$$

Thus, the maximum electron-neutrino energy is $E_\nu^{max} \approx 52.8 \text{ MeV}$. In the case of muon neutrinos the energy distribution is different. In refs. [12,13], a muon-neutrino energy distribution is presented in which $E_\nu^{max} \approx 280.0 \text{ MeV}$.

For comparison of the theoretical cross sections with experimental data we define the flux averaged cross section $\bar{\sigma}$ by

$$\bar{\sigma} = \frac{\int_0^{E_\nu^{max}} \sigma(E_\nu) W(E_\nu) dE_\nu}{\int_0^{E_\nu^{max}} W(E_\nu) dE_\nu} \quad (10)$$

The numerator of eq. (10) represents the folding of the neutrino cross section with the appropriate energy distribution. The denominator stands for normalization requirements.

5 Discussion of the results

There are few experimental data to compare with in this energy regime. One of the reactions for which there are measurements is the ν_e cross section on ^{12}C both from the KARMEN collaboration [8,9] and Los Alamos [10,11]. The cross sections are the averaged ones with the Michel distribution, and although there are still some discrepancies in the amount of strength that goes into the excitation of the $^{12}N(gs)$ and the excited states, the total ν_e cross section is about the same in both experiments (see table 3). In the present work, using the modified method, we have found that, $\bar{\sigma} = 0.14 \times 10^{-40} \text{ cm}^2$, which agrees well with experiments. In ref. [5] a thorough discussion of the results of other methods has been done.

Recently, there have been some measurements in ^{127}I at Los Alamos obtained by experiments of radiochemical type. This means that the ^{127}Xe in the final state is chemically separated. Hence, this kind of experiment includes all final states in which the ground state of ^{127}Xe or any excited state of this element (which will go to the ground state by radiative decay) are produced.

In table 3 we have computed the ν_e cross sections averaged over the Michel distribution for several nuclei and we show results of the total and radiochemical cross sections. The ^{12}N nucleus has a very low proton emission threshold which makes it unsuitable for radiochemical experiment, but all the other nuclei quoted in the table 3 can in principle qualify for such an experiment and we have evaluated this cross section.

Table 3. Flux averaged cross section $\bar{\sigma}$ for ν_e obtained by folding the cross section σ in a Michel neutrino energy distribution (see text). $\bar{\sigma}_{rad}$ contains the contribution of particle bound states only and $\bar{\sigma}_{tot}$ contains the contribution of all accessible particle states of the final nucleus.

Reaction	$\bar{\sigma}_{tot}$	$\bar{\sigma}_{rad}$	KARMEN Exp.	LAMPF Exp.
$^{12}_6 C(\nu_e, e^-)^{12}_7 N$	0.14	-	0.15 ± 0.03 ref. [9]	$0.14 \pm .03$ ref. [10]
$^{37}_{17} Cl(\nu_e, e^-)^{37}_{18} Ar$	1.8	1.4		
$^{40}_{18} Ar(\nu_e, e^-)^{40}_{19} K$	1.9	1.3		
$^{71}_{31} Ga(\nu_e, e^-)^{71}_{32} Ge$	4.0	2.7		
$^{81}_{35} Br(\nu_e, e^-)^{81}_{36} Kr$	4.5	3.2		
$^{98}_{42} Mo(\nu_e, e^-)^{98}_{43} Tc$	5.3	2.7		
$^{115}_{49} In(\nu_e, e^-)^{115}_{50} Sn$	7.2	4.7		
$^{127}_{53} I(\nu_e, e^-)^{127}_{54} Xe$	7.3	4.3		6.2 ± 2.5 ref. [11]*
$^{205}_{81} Tl(\nu_e, e^-)^{205}_{82} Pb$	14.0	6.3		

* This experiment is of radiochemical type.

We can compare our results with those of the recent radiochemical experiment at LAMPF [11] for ^{127}I . The experimental results quoted in [11] give a cross section of

$$\bar{\sigma} = (6.2 \pm 2.5) \times 10^{-40} \text{ cm}^2$$

We get a value of

$$\bar{\sigma} = 4.2 \times 10^{-40} \text{ cm}^2$$

for this cross section. It is also interesting to compare our results with two other recent theoretical results. On the one hand, in ref. [22] the values

$$\bar{\sigma} = 6.4 \times 10^{-40} \text{ cm}^2 \quad \text{and} \quad \bar{\sigma} = 3.0 \times 10^{-40} \text{ cm}^2$$

are quoted using two different approaches, which rely both on the closure approximation. We should recall, however, that these are total cross sections and not radiochemical. They should be compared to our results in table 3 of $\bar{\sigma} = 7.3 \times 10^{-40} \text{ cm}^2$.

On the other hand, in ref. [3] the authors evaluate a genuine radiochemical cross section by summing over the discrete excited states of ^{127}Xe . They obtain a cross section of $\bar{\sigma} = 2.1 \times 10^{-40} cm^2$, if $g_A = -1.0$ is used, or $\bar{\sigma} = 3.1 \times 10^{-40} cm^2$, if $g_A = -1.26$ is used. Our method provides an automatic renormalization of g_A by means of the ph and Δh RPA excitation which leads to quenched values of g_A [20]. Hence, the results of ref. [3], are about a factor of two smaller than ours.

There is another recent experimental information which can be contrasted with our predictions. In a recent experiment at Los Alamos with muon neutrinos [13], they obtain the cross section

$$\bar{\sigma} = [8.3 \pm (stat.) \pm 1.6(syst.)] \times 10^{-40} cm^2$$

averaged over the ν_μ flux in the range of $123.7 < E_\nu < 280 MeV$ for the $^{12}C(\nu_\mu, \mu^-)X$ reaction. Averaging over the same distribution we obtain a cross section of $\bar{\sigma} = 19 \times 10^{-40} cm^2$. We should recall that this experiment corrects considerably the previous data of ref. [12]. Our values here are a bit smaller than the $\bar{\sigma} = 25 \times 10^{-40} cm^2$ quoted in ref. [5], because the ν_μ distribution of ref. [13] has less strength at high energies than the one quoted in [12], which was used to evaluate the results of ref. [5]. It is also interesting to compare these results with another recent theoretical calculation [23] which uses a continuum random phase approximation calculation and which provides the value $\bar{\sigma} = 20 \times 10^{-40} cm^2$.

6 Summary and conclusions

In the present work we have studied the charged current neutrino and antineutrino nucleus inclusive and semi-inclusive cross sections for low and intermediate energies $20 MeV \leq E_\nu \leq 500 MeV$. We have chosen a set of eight nuclei which are very important from an experimental point of view in ongoing experiments and current proposals. The method used is reliable and considerably easier technically than other accurate methods and can be used to make further predictions in other isotopes of interest.

We made comparisons of our results with existing data on inclusive cross sections for the $^{12}C(\nu_e, e^-)X$ reaction measured at LAMPF and KARMEN, and the agreement is good. We also made a comparison with a recent radiochemical experiment for the $^{127}I(\nu_e, e^-)^{127}Xe$ reaction and found our results to be compatible with experiment within experimental errors. On the other hand, the cross section for the $^{12}C(\nu_\mu, \mu^-)X$ reaction, which we obtain, is about a

factor of two bigger than that of a recent experiment at LAMFF and essentially equal to other recent theoretical calculations for the same reaction.

Although, discrepancies like the above with experiment still remain, more serious disagreements found in the past, have been overcome with the advent of new refined experiments. This strengthens our confidence in the method used and makes the predictions made here for different nuclei a very valuable information to be used in future experiments or in the calibration of new neutrino detectors.

Acknowledgements: We would like to acknowledge support from the EU Human Capital and mobility Program CHRX-CT 93-0323 and one of us (E.O.) from the Humboldt Foundation. This work has been partially supported by CICYT contract number AEN-93-1205.

References

- [1] R. Davis, *Prog. Part. Nucl. Phys.* **32**, 13, (1994) and references therein.
- [2] R. S. Raghavan, *Phys. Rev. Lett.* **37**, 259, (1976);
J. N. Bahcall *et al.*, *Phys. Rev. Lett.* **40**, 1351, (1978).
- [3] J. Engel, S. Pittel and P. Vogel, *Phys. Rev. Lett.* **67**, 426, (1991); *Phys. Rev. C* **50**, 1702, (1994).
- [4] T.S. Kosmas and E. Oset, *Phys. Rev. C* , to be published.
- [5] S. K. Singh and E. Oset, *Phys. Rev. C* **48**, 1246, (1993); *Nucl. Phys. A* **542**, 587, (1992).
- [6] A. I. Abazov *et al.*, *Phys. Rev. Lett.* **67**, 3332, (1991);
P. Anselmann *et al.*, *Phys. Lett. B* **285**, 376, (1992);
K. S. Hirata *et al.*, *Phys. Rev. Lett.* **63**, 16, (1989).
- [7] J. Rapaport *et al.*, *Phys. Rev. Lett.* **47**, 1518, (1981); **54**, 2325, (1985);
D. Krfcheck *et al.*, *Phys. Rev. Lett.* **55**, 1051, (1985); *Phys. Lett. B* **189**, 299, (1987);
Yu.S. Lutostansky and N.B. Skul'gina, *Phys. Rev. Lett.* **67**, 430, (1991).
- [8] B. Bodmann *et al.*, *Phys. Lett. B* **280**, 198, (1992).
- [9] B. Zeitnitz, *Prog. Part. Nucl. Phys.* **32**, 351, (1994).
- [10] D.A. Krakauer *et al.*, *Phys. Rev. C* **45**, 2450, (1992).

- [11] B.T. Cleveland, T. Daily, J. Distel, K. Lande, C.K. Lee et al., in Proceedings of the 23rd International Cosmic Ray Conference (University of Calgary, Alberta, Canada, July 17-18, 1993), edited by D.A. Leahy, R.B. Hicks, and D. Venkatesan, World Scientific, (1993), Vol. 3, p. 865.
- [12] D. D. Koetke et al., Phys. Rev. **C 46**, 2554, (1992).
- [13] M. Albert et al., Phys. Rev. **C 51**, R1065, (1995).
- [14] B. Goulard and H. Primakoff, Phys. Rev. **135**, B1139, (1964);
 J. S. Bell and C. H. Llewellyn-Smith, Nucl. Phys. **B 28**, 317, (1971);
 T. W. Donnelly and J. D. Walecka, Phys. Lett. **B 41**, 275, (1972);
 E. V. Bugaev et al., Nucl. Phys. **A 324**, 350, (1979).
- [15] T. Kuramoto, M. Fukugita, Y. Kohyama and K. Kubodera, Nucl. Phys. **A 512**, 711, (1990).
- [16] T. S. Kosmas and E. Oset, Proc. 5th Hellenic Symp. on Nucl. Phys., (Patras, Greece, 6-7 May, 1994), ed. K. Syros and C. Ronchi, Advances in Nucl. Phys. EUR 16302 (1995) 29-41.
- [17] E. Oset, D. Strottman, H. Toki, and J. Navarro, Phys. Rev. **C 48**, 2395, (1993).
- [18] A.L. Fetter and J. D. Walecka, Quantum Theory of Many Particle Systems (McGraw Hill, N.Y. 1971).
- [19] H. C. Chiang, E. Oset and P. Fernandez de Cordoba, Nucl. Phys. **A 510**, 591, (1990);
 H. C. Chiang, E. Oset, R. C. Carrasco, J. Nieves and J. Navarro, Nucl. Phys. **A 510**, 573, (1990).
- [20] E. Oset and M. Rho, Phys. Rev. Lett. **42**, 47, (1979).
- [21] E. Oset, P. Fernandez de Cordoba, L.L. Salcedo and R. Brockmann, Phys. Reports **188**, 79, (1990).
- [22] S. L. Mintz and M. Pourkaviani, Nucl. Phys. **A 584**, 665, (1995).
- [23] E. Kolbe, K. Langanke, and S. Krewald, Phys. Rev. **C 51**, 1122, (1995).